Shear Coaxial Jets Subjected to an External Acoustic Field

Ivett A. Leyva[*], Doug Talley[*], Sophonias Teshome[+], Juan Rodriguez[^], Jeffrey Graham[^]
[*]Air Force Research Laboratory, AFRL, Edwards AFB, CA, USA
[+]AFRL/UCLA Los Angeles, CA, USA
[^] Formerly at AFRL Edwards, AFB, CA, USA

1 Introduction

Shear coaxial injectors are a common design choice for boost and upper stage cryogenic rocket engines where the propellants are liquid oxygen and hydrogen. The liquid oxygen is generally introduced as the inner jet and hydrogen is introduced in the coaxial or outer jet. Mixing between the inner and outer jet happens through the shear layer that develops in the interface of the two propellants; the faster the shear layer grows the faster mixing occurs. To provide good mixing, shear coaxial jets depend on a large difference in the velocities and momentum fluxes of the two streams, which is easily achieved in rocket engines. High performance for rocket engines is also coupled to higher chamber pressures. For example, the F-1 engine for the Saturn V operated at 6.7 MPa [1] while the SSME engine operates at 19.3 MPa [2]. One consequence of operating at higher pressures is that the propellants are injected at pressures greater than their individual critical pressures. In the case of hydrogen it is usually injected at higher than its critical temperature, so it is considered a supercritical fluid, whereas oxygen usually is injected at lower than its critical temperature, so it is considered a liquid-like or transcritical fluid. What happens to the mixing processes in a shear coaxial injector as the working fluids cross into the supercritical regime is the first topic of this paper. The second topic is how the mixing reacts to external acoustics. The interest on knowing the response to acoustics arises from the ever present concern of developing combustion instabilities on a new engine design or new operating conditions. The results presented here are solely concerned with all-nitrogen shear coaxial injectors exiting into a nitrogen atmosphere. This choice allows us to have a single critical point making it easy to know exactly the thermodynamic state of the inner and outer jets and the chamber. Being non-reacting allows us to focus on the fluid mechanic instabilities of a coaxial jet and their response to external acoustics.

2 Experimental Setup

The Cryogenic Supercritical Laboratory (EC-4) at the Air Force Research Laboratory, Edwards Air Force Base, CA, where the experiments are performed, is shown in Fig. 1. The photograph shows the test chamber in the center with one acoustic driver on each side and a high speed camera on the front. Details from the acoustic drivers are also shown. The injector flow is from top to bottom. The maximum chamber pressure is 13.8MPa. The lowest tested temperature is about 95K. Nominal injector flow rates are in the order of g/s. This is a non-reacting facility using only N_2 for the pressurizing gas and for the injector flows. In order to maximize the effect of the available acoustic energy on the jet, a rectangular inner chamber was created into which the injector flow exits and the acoustic waves are directed. The inner chamber has a height of 6.6 cm, a width of 7.6 cm and a depth of 1.3 cm. The top of the inner chamber consists of a perforated plate to allow the outer and inner chambers to get their pressures equalized. Both the top and bottom pieces have an orifice at their centers. The top plate's orifice allows the coaxial injector tip to enter the inner chamber and the bottom orifice provides an exit for the flow. The bottom orifice is also used to introduce a thermocouple and high speed pressure transducer to study the properties of the flow near the jet exit plane. The front and back sides to the inner chamber are plexiglass for flow visualization. On the back plexiglass panel, there are three Kulite high speed pressure transducers, equally spaced, just above the exit plane of the coaxial injector to measure the acoustic pressure field. The outer and inner jets are

Correspondence to: ivett.leyva@edwards.af.mil

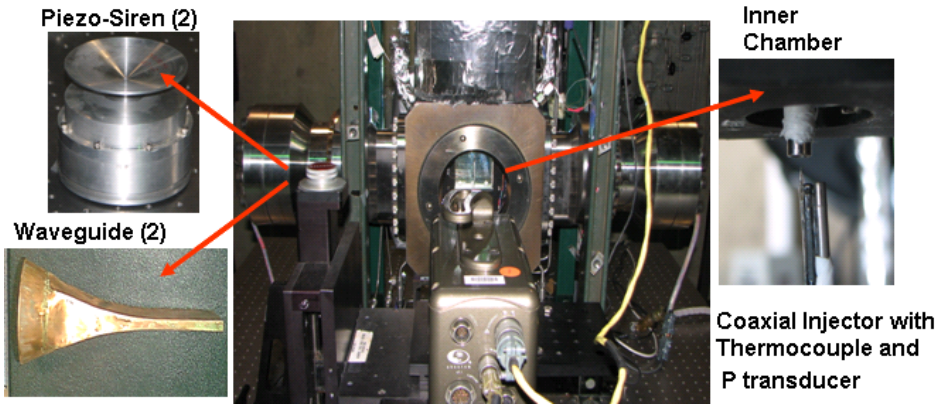

Figure 1. Experimental Cell EC-4 at AFRL, Edwards, CA.

cooled by independent heat exchangers (HEs) using liquid N_2 (LN2) as the coolant. The temperatures of the two jets are controlled by the flow rate of LN2 through the HE's. The mass flow rates for the inner and outer jets are measured with Porter mass flow meters (models 122 and 123-DKASVDAA) before they are cooled, since it is easier to measure mass flow rates at ambient temperature than at cryogenic conditions. The two acoustic sources are nominally identical and use a piezosiren to generate acoustics waves at frequencies of about 3kHz and 5.2kHz. A waveguide is used to guide the acoustic waves from a round cross section at the source to a rectangular cross-section at the inner chamber.

3 Injector Geometry and Measurement Techniques

Two injector geometries will be discussed in this paper. Pictures of two representative geometries are shown in Fig. 2. The injector on the left has a thick inner jet post (t/d=1.06) and the one on the right has a thin post (t/d=0.089). Together, they give us a practical upper and lower limit for the inner jet thickness. For the thick post injector, the L/D was 100 for the inner jet and 34 for the outer jet (taking as reference the hydraulic diameter). The same ratios were 65 and 55 respectively for the thin post injector. The inner and outer injector flows are designed to be fully developed turbulent. For the cases studied the inner jet can be flushed or recessed with respect to the outer jet.

The flows are characterized with different measurements aside from static pressure and flow rates. Temperature profiles of the inner and outer jets are taken at the exit plane of the injector with an unshielded type E thermocouple with a bead diameter of 0.1 mm. The thin post injector is equipped with high speed pressure transducers and thermocouples in both the inner and outer jet reservoirs. Three high speed pressure transducers are also placed at the exit plane of the injector. Finally, a Phantom 7.1 high speed camera is used to obtain backlit movies at frame rates of 20-40 kHz. The sizes of the images presented here vary from 128×224 to 196×400 pixels. Each pixel represents an area of approximately 0.08×0.08 mm.

4 Baseline measurements without acoustics

Studies of non-reacting shear coaxial mixing date back to the 60's with the pioneering paper of Chigier and Beer [3] using air-air coaxial jets at atmospheric pressure. They concluded that the inner jet potential core decreased as the outer to inner velocity ratio increased. The potential core is associated with the inner jet volume not entrained into the shear layer formed between the inner and outer jets. Ko et al [4-6], also studying air jets, have made a wealth of contributions since the 70's

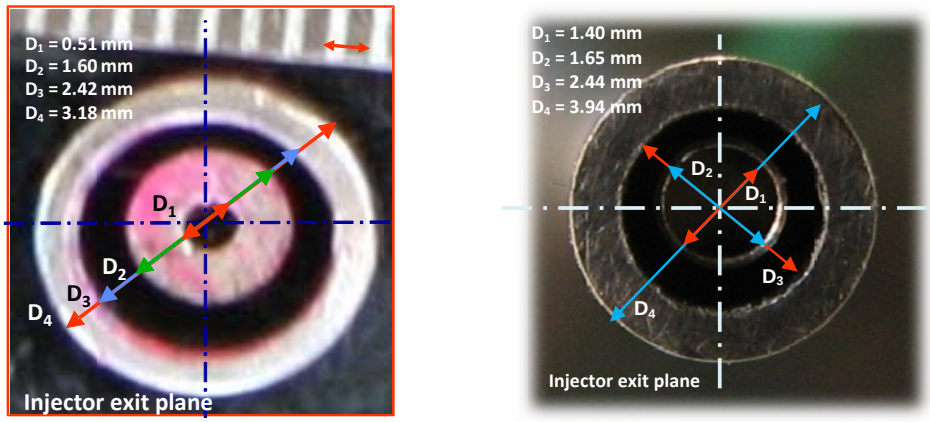

Figure 2. Geometries of two injectors tested. Left: thick post injector. Right: thin post injector.

describing the observed structures and mixing phenomena, pertaining mainly to the near field. Dahm et al [7], using water coaxial jets, investigated the vortical structures formed in the shear layers as a function of the velocity ratio and pointed out the effect of the different types of vortical structures on the inner jet core length. Villermeaux [8] and other researchers cited on the review article by Lasheras and Hopfinger [9] deduced that for shear coaxial jets, the outer to inner jet momentum flux ratio, J, defined as $\rho_o u_o^2 / \rho_i u_i^2$, where o refers to outer and i to inner jet, is a dominant non-dimensional parameter characterizing mixing. As J increases the mixing becomes more efficient and the inner jet is entrained by the outer jet within a shorter distance.

Figure 3 shows a compilation of available data on coaxial jets presented by Davis [10] with more recent results added for from Leyva et al. [11]. The dark core, intact core, or potential core length is plotted as a function of J. As Davis [10] points out, two braches emerge from the data. The upper branch corresponds to two phase flows and the lower one to single phase flows which include gas-gas, supercritical-supercritical, and supercritical-transcritical. It is evident that both branches scale with J, but because of the large bands where the data falls, further analysis is underway to investigate if incorporating other non-dimensional parameters, such as velocity ratio can collapse the experimental data even further.

5 Effects of Acoustics on Thick Post Injector

The general trends of the behavior of the thick post injector are shown in Fig. 4. The set of images on the left correspond to a subcritical pressure where the inner jet is liquid and the outer jet is gas, and the set of images on the right correspond to a supercritical pressure. The momentum flux ratio J spans about two orders of magnitude. The top row corresponds to cases without acoustic excitation. The middle row corresponds to cases with acoustics turned on where the jet is in a pressure antinode. The bottom row corresponds to cases with the jet in a pressure node.

Attention may be directed first to the subcritical cases on the left side of Fig. 4. As previously reported [10-11] and can be seen in Fig. 4, the dark core decreases as J increases. However, we can also see that at high J values, the inner jet appears to be much thicker at the exit plane. This is because, above certain critical value of J, a recirculation bubble is established downstream of the inner jet, much like Villermeaux [12] had observed in water jets. Also observe that acoustics shorten the inner jet at the lower value of J without undulation. However, undulation becomes prominent at J=2.6 and J=9.6. Undulation of the jet is almost intuitive as we think of the transverse acoustic field imposing a lateral force on the jet, the direction of which oscillates as the acoustic cycle proceeds. The effects look more

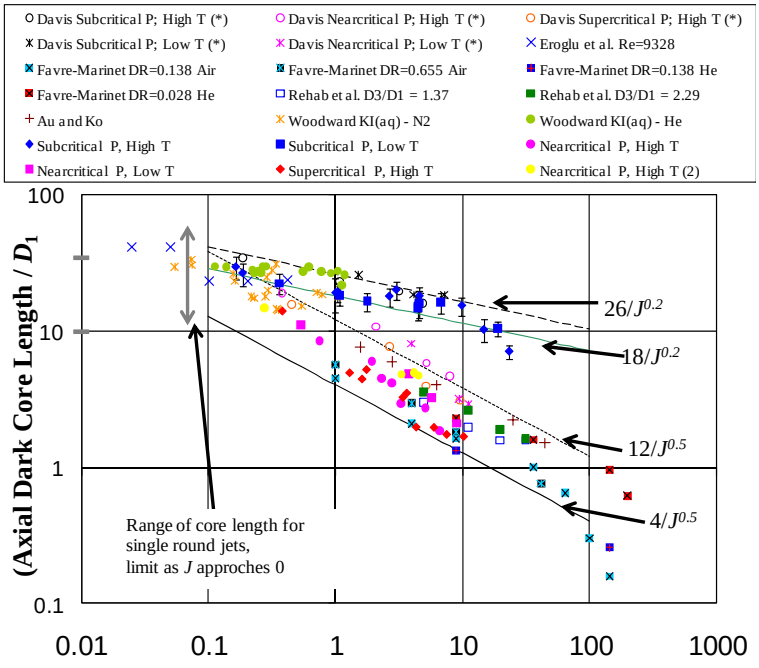

Figure 3. Scaling of dark core length of shear coaxial jets with momentum flux ratio.

dramatic for the middle value of J since the dark core for that case has enough length to sustain several undulations before it breaks. The undulation effect is greatest at a velocity antinode and moderate J values. Attention may be directed next to the supercritical cases on the right side of Fig. 4. The set of images on the right correspond to supercritical pressures. For the first two cases, the inner jet is at transcritical conditions whereas for the last case (J=9.3) the inner jet temperature is higher than the critical temperature. The trends are qualitatively similar to the subcritical cases, with the caveat that the dark core is shorter for a given value of J (see also Fig. 3) and so the undulations are not as pronounced for mid values of J. Also, the natural inner jet instabilities for the baseline cases are more prominent for the higher pressure case. Finally, the inner jet is so short for the supercritical case J=9.3 that the acoustics have the effect of bending the core from left/right as the cycle proceeds. A more detailed analysis will be presented for this geometry and compared with a similar analysis for the thin post injector.

6 Cycle-to-cycle and averaged analysis of coaxial jets

By synchronizing the movie frames and the high speed transducers we can obtain cycle-to-cycle information on how the jet reacts to the acoustic field. Fig. 5 shows a snapshot of the backlit images together with the pressure measured at the inner and outer jet reservoirs and directly behind the coaxial injector. By comparing the relative amplitude of the signals we can assess whether the acoustics are being damped or amplified at the injector reservoirs, which is particularly useful when trying to understand coupling of the post modes with the external acoustics. Also, one can examine the behavior of the jet at pressure nodes and antinodes. FFT's of the different signals are also performed to determine characteristic frequencies for the system. This type of analysis will be presented for the thin post injector and at least one more new geometry.

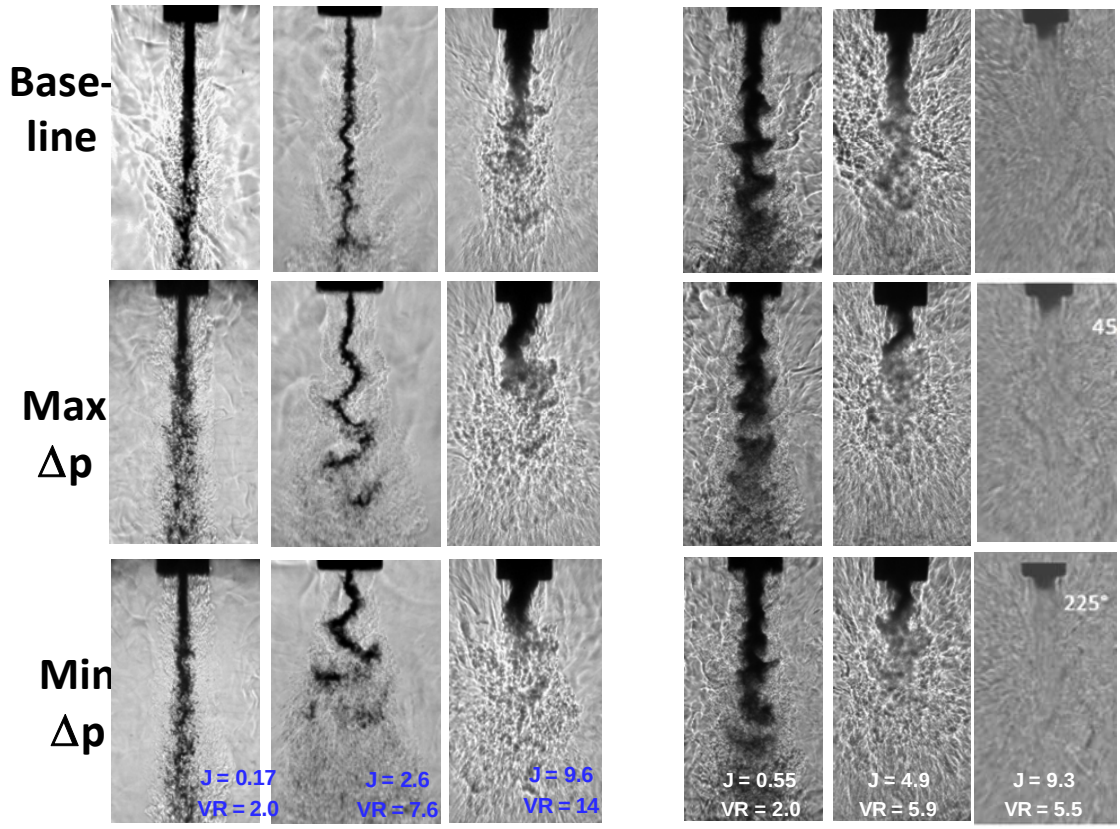

Figure 4. Behavior of shear coaxial jets at baseline conditions (without acoustics) and exposed to acoustic pressure nodes and antinodes. Left: Subcritical pressure (Pr=0.45). Right: Supercritical pressure (Pr=1.05).

Finally, very careful measurements of the exit plane temperature for a range of conditions will be presented. Fig. 6 shows a sample. The differences on the reservoir and exit plane temperatures for the

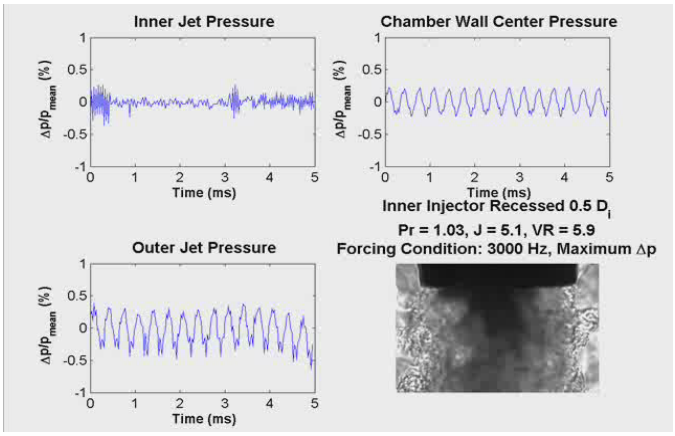

Figure 5. Synchronized close-up image of injector flow and acoustic pressure fields.

inner and outer jets are indicative of the heat transfer taking place along the injector and can be assessed as a function of J and velocity ratio. The growth of the shear layer between the inner and outer jet can also be studied by looking at these temperature profiles.

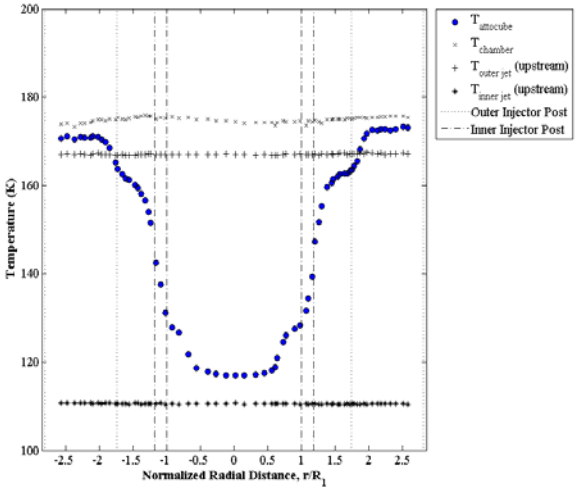

Figure 6. Relevant temperature profiles measured upstream and downstream of the injector exit plane.

References

[1] http://history.msfc.nasa.gov/saturn_apollo/documents/F-1_Engine.pdf

[2] JPP Vol. 18, No. 2, March–April 2002

[3] Chigier, NA and Beer JM. (1964). The flow region near the nozzle in double concentric jets. Trans. ASME 86D, J. of Basic Engineering. 4:797-804.

[4] Kwan, ASH and Ko, NWM. (1976). Coherent structures in subsonic coaxial jets. J of Sound and Vibration. 48(2):203-219.

[5] Ko, NWM and Au, H. (1985). Coaxial jets on different mean velocity ratios. J of Sound and Vibration. 100(2):211-232.

[6] Kwan, ASH and Ko, NWM. (1977). Covariance measurements in the initial region of coaxial jets. J of Sound and Vibration. 52(4):567-578.

[7] Dahm, W., Frieler, C., Tryggvason, G. (1992). Vortex Structure and Dynamics in the Near Field of a Coaxial Jet. J. of Fluid Mechanics. 241:371-402.

[8] Lasheras, JC, Villermaux, E and Hopfinger EJ. (1998). Break-up and atomization of a round water jet by a high-speed annular air jet. J. of Fluid Mechanics. 357:351–379.

[9] Villermaux, E. and Rehab, H. (2000). Mixing in coaxial jets. J. of Fluid Mechanics. 425:161–185.

[10] Davis, DW. (2006). On the Behavior of a Shear-Coaxial Jet, Spanning Sub- to Supercritical Pressures, With and Without an Externally Imposed Transverse Acoustic Field. Ph. D. Dissertation: Dept. of Mech. and Nuclear Engineering, Pennsylvania State University.

[11] Leyva, I. A., Chehroudi, B., Talley, D. (2007). Dark-Core Analysis of Coaxial Injectors at Sub-, Near-, and Supercritical Conditions in a Transverse Acoustic Field. AIAA 2007- 5456.

[12] Villermaux, E., Rehab, H., and Hopfinger, E. J. (1994). Breakup Regimes and Self-Sustained Pulsations in Coaxial Jets. Meccanica. 29:393-401.